optica

# Enhancing photon correlations through plasmonic strong coupling

R. Sáez-Blázquez,[1] J. Feist,[1] A. I. Fernández-Domínguez,[1,3] and F. J. García-Vidal[1,2,4]

[1]Departamento de Física Teórica de la Materia Condensada and Condensed Matter Physics Center (IFIMAC), Universidad Autónoma de Madrid, E-28049 Madrid, Spain
[2]Donostia International Physics Center (DIPC), E-20018 Donostia/San Sebastián, Spain
[3]e-mail: a.fernandez-dominguez@uam.es
[4]e-mail: fj.garcia@uam.es

Received 27 June 2017; revised 21 September 2017; accepted 2 October 2017 (Doc. ID 301188); published 1 November 2017

**There is an increasing scientific and technological interest in the design and implementation of nanoscale sources of quantum light. Here, we investigate the quantum statistics of the light scattered from a plasmonic nanocavity coupled to a mesoscopic ensemble of emitters under low coherent pumping. We present an analytical description of the intensity correlations taking place in these systems and unveil the fingerprint of plasmon-exciton-polaritons in them. Our findings reveal that plasmonic cavities are able to retain and enhance excitonic nonlinearities, even when the number of emitters is large. This makes plasmonic strong coupling a promising route for generating nonclassical light beyond the single-emitter level.** 

***OCIS codes:*** (240.6680) Surface plasmons; (240.5420) Polaritons; (140.6630) Superradiance, superfluorescence; (350.4238) Nanophotonics and photonic crystals; (030.5290) Photon statistics; (270.0270) Quantum optics.

https://doi.org/10.1364/OPTICA.4.001363

## 1. INTRODUCTION

Much research attention has focused lately on plasmonic nanocavities for strong coupling applications. In these devices, the interaction between surface plasmons (SPs) and quantum emitters (QEs) can be intense enough to yield new hybrid light–matter states, the so-called plasmon-exciton-polaritons (PEPs) [1]. PEPs involving macroscopic QE ensembles have been reported in planar [2–4] and nanoparticle [5–7] geometries, and they have been used for controlling chemical reactions [8,9] or enhancing charge/energy transport [10,11]. From a purely photonics perspective, room-temperature PEP lasing has been recently reported [12,13]. However, in order to harness the full potential of plasmonic cavities for quantum optical applications, plasmonic systems that display nonlinearities at the single-photon level would be highly desirable [14]. This is not possible in macroscopic ensembles, which present collective boson-like behavior at pumping levels below the QE saturation regime [15].

Very recently, strong coupling signatures in the power spectrum of nanogap metallic cavities filled with only a few QEs have been reported [16,17]. These experimental advances have been accompanied by theoretical efforts aiming to clarify the near-field conditions yielding PEPs at the single-emitter level [18]. However, the generation of nonclassical light through plasmonic strong coupling has not been explored yet. In this paper, we fill this gap by investigating the quantum statistics of the photons scattered by a nanocavity strongly coupled to a mesoscopic emitter ensemble (up to ∼100 QEs) under coherent pumping. We develop an analytical description of the quantum optical properties of the system that allows us to reveal that, contrary to what is expected, plasmonic cavities enhance photon correlations in QE ensembles of considerable size under strong coupling conditions.

## 2. MODEL

Figure 1 depicts the system under study: $N$ identical QEs with transition dipole moment $\boldsymbol{\mu}_{\mathrm{QE}}$ and frequency $\omega_{\mathrm{QE}}$ interact with the near-field $\mathbf{E}_{\mathrm{SP}}$ (the same for all QEs) of a single SP mode of energy $\omega_{\mathrm{SP}}$ supported by a generic nanocavity. Both subsystems undergo radiative and nonradiative damping, with decay rates $\gamma_{\mathrm{QE/SP}} = \gamma^{\mathrm{r}}_{\mathrm{QE/SP}} + \gamma^{\mathrm{nr}}_{\mathrm{QE/SP}}$. We consider QEs in which pure dephasing is negligible as this process would suppress quantum correlations in the emitted photons. Both QEs and SPs are coherently driven by a laser field $\mathbf{E}_{\mathrm{L}}$ with frequency $\omega_{\mathrm{L}}$. The steady-state density matrix $\hat{\rho}$ for the hybrid system is the solution of the Liouvillian equation ($\hbar = 1$)

$$i[\hat{\rho}, \hat{H}] + \frac{\gamma_{\mathrm{SP}}}{2}\mathcal{L}_{\hat{a}}[\hat{\rho}] + \frac{\gamma^{\mathrm{r}}_{\mathrm{QE}}}{2}\mathcal{L}_{\hat{S}^-}[\hat{\rho}] + \frac{\gamma^{\mathrm{nr}}_{\mathrm{QE}}}{2}\sum_{i=1}^{N}\mathcal{L}_{\hat{\sigma}_i}[\hat{\rho}] = 0, \quad (1)$$

where $\hat{a}$, $\hat{\sigma}_i$, and $\hat{S}^- = \sum_{i=1}^{N}\hat{\sigma}_i$ are the annihilation operators for the SP mode, the $i$th QE, and the ensemble superradiant state, respectively. The damping associated with operator $\hat{O}$ is described by standard Lindblad superoperator $\mathcal{L}_{\hat{O}}[\hat{\rho}] = 2\hat{O}\hat{\rho}\hat{O}^{\dagger} - \{\hat{O}^{\dagger}\hat{O}, \hat{\rho}\}$. Equation (1) reflects that, contrary to nonradiative decay, radiation damping is a coherent process that involves only the

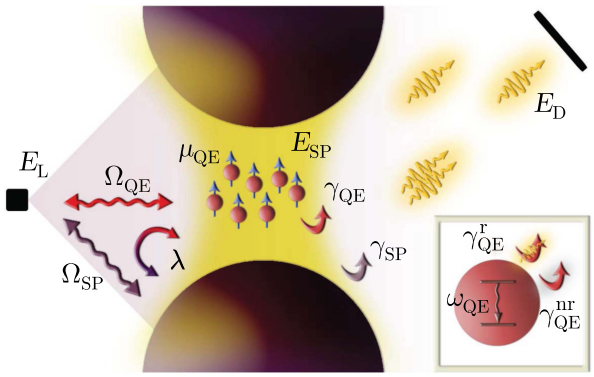


**Fig. 1.** QE ensemble resonantly coupled to a generic plasmonic cavity. The right inset depicts the two-level QE model.

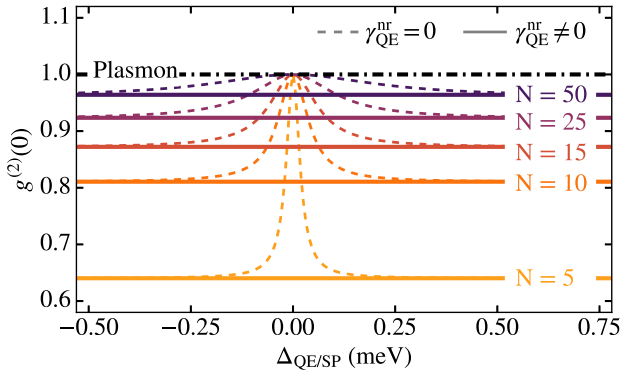


**Fig. 2.** Correlation function $g^{(2)}(0)$ versus laser detuning for SP (black dashed–dotted line) and QEs (colored lines) uncoupled. Various ensemble sizes are shown, with (solid) and without (dashed) the inclusion of QE nonradiative decay, $\gamma^{nr}_{QE}$.

superradiant state of the QE ensemble (the rest of the ensemble states are dark). In the rotating frame, the coherent dynamics is governed by the time-independent Tavis–Cummings Hamiltonian [19]

$$\hat{H} = \Delta_{SP}\hat{a}^\dagger\hat{a} + \Delta_{QE}\hat{S}_z + \lambda(\hat{S}^+\hat{a} + \hat{S}^-\hat{a}^\dagger) + \Omega_{SP}(\hat{a}^\dagger + \hat{a}) + \Omega_{QE}(\hat{S}^+ + \hat{S}^-), \quad (2)$$

with $\Delta_{QE/SP} = \omega_{QE/SP} - \omega_L$ and $\hat{S}_z = \frac{1}{2}[\hat{S}^+, \hat{S}^-]$. The QE–SP coupling is $\lambda = \mathbf{E}_{SP}\cdot\boldsymbol{\mu}_{QE}$, while $\Omega_{QE} = \mathbf{E}_L\cdot\boldsymbol{\mu}_{QE}$ and $\Omega_{SP} = \mathbf{E}_L\cdot\boldsymbol{\mu}_{SP}$ are the pumping frequencies. Here, $\boldsymbol{\mu}_{SP}$ is the effective SP dipole moment. Once the steady-state density matrix is known, the first- and second-order correlation functions can be calculated from the scattered far-field operator at the detector $\hat{\mathbf{E}}^-_D \propto \boldsymbol{\mu}_{SP}\hat{a}^\dagger + \boldsymbol{\mu}_{QE}\hat{S}^+$. Note that we have taken advantage of the subwavelength dimensions of the system to neglect the differences between the electromagnetic Green's function describing the emission from the SP and the various QEs in $\hat{\mathbf{E}}^-_D$.

## 3. RESULTS AND DISCUSSION

Before investigating photon correlations under strong coupling conditions, we consider first both SP and QE subsystems uncoupled. For this purpose, we solve Eq. (1) numerically and compute the normalized zero-delay second-order correlation function in the steady state $g^{(2)}(0) = \langle\hat{\mathbf{E}}^-_D\hat{\mathbf{E}}^-_D\hat{\mathbf{E}}^+_D\hat{\mathbf{E}}^+_D\rangle/\langle\hat{\mathbf{E}}^-_D\hat{\mathbf{E}}^+_D\rangle^2$. This magnitude measures the intensity fluctuations of the emitted light and is related to the probability for two photons to arrive at the same time at the detector. Values of $g^{(2)}(0)$ smaller than 1 indicate antibunching, which cannot be achieved with classical light [20]. We only consider low laser intensities and study quantum correlations far from the pumping regime in which QE saturation becomes relevant. Figure 2 plots $g^{(2)}(0)$ as a function of the laser detuning for an empty plasmonic cavity (black dashed–dotted line) and ensembles of different number of emitters (colored solid lines). For comparison, the correlation spectra for QEs with $\gamma^{nr}_{QE} = 0$ are also shown (colored dashed lines). The parameters modeling the single SP mode are $\omega_{SP} = 3$ eV, $\gamma_{SP} = 0.1$ eV, and $\mu_{SP} = 19$ e·nm [5]. Our calculations yield $g^{(2)}(0) = 1$, as expected from the SP inherent bosonic character. For proof-of-principle purposes, we have chosen QE parameters as $\omega_{QE} = 3$ eV, $\gamma^r_{QE} = 6$ μeV ($\mu_{QE} = 1$ e·nm), and $\gamma^{nr}_{QE} = 15$ meV. These values correspond to organic molecules that display very low quantum yield and in which collective strong coupling has been already reported [3,13].

As we show below, these types of QEs are also favorable for generating photon correlations. Notice then that for a practical realization of our findings with organic QEs, the experiments should be carried out at low temperature in order to avoid pure dephasing processes inside the QEs. For all $N$, photon statistics are sub-Poissonian ($g^{(2)}(0) < 1$), but the degree of antibunching decreases rapidly with the ensemble size. As $N$ increases, the system bosonizes and the quantum character of the scattered light is lost [note that $g^{(2)}(0) = 0.96$ for $N = 50$]. Neglecting nonradiative damping only leads to an extremely narrow Lorentzian-like profile, which suppresses antibunching exactly at zero detuning. This observation is in agreement with the resonance fluorescence phenomenology of a single QE [21], in which no incoherent scattering occurs in the limit of vanishing pumping (saturation effects in the QE population are negligible). Note that the $g^{(2)}(0)$ behavior obtained from our model is in accordance with more sophisticated descriptions [22] of QE ensembles.

Exact numerical solutions to Eq. (1) can be obtained for strong QE–SP coupling. However, such calculations are only possible for configurations involving very small QE ensembles [23], even far from the QE saturation regime [24]. In order to circumvent this limitation and explore photon statistics in mesoscopic ensembles, we map Eq. (1) into the effective non-Hermitian Hamiltonian [25]

$$\hat{H}_{eff} = \hat{H} - i\frac{\gamma_{SP}}{2}\hat{a}^\dagger\hat{a} - i\frac{\gamma^{nr}_{QE}}{2}\hat{S}_z - i\frac{\gamma^r_{QE}}{2}\hat{S}^+\hat{S}^-, \quad (3)$$

where $\hat{H}$ is given by Eq. (2). Note that $\hat{H}_{eff}$ depends only on the collective bright-state operators of the QEs and is independent of the dark states of the ensemble (superpositions of QE excitations that do not couple to the plasmon or external light), which means a drastic reduction in the Hilbert space for large $N$. Equation (3) results from neglecting the refilling terms $\hat{O}\hat{\rho}\hat{O}^\dagger$ in the Lindblad superoperators in Eq. (1). This approach can be safely employed in the regime of low pumping, where the ground state can be considered as a reservoir with population equal to 1. In this limit, we can solve the Schrödinger equation for $\hat{H}_{eff}$, treating the coherent driving, $E_L$, as a perturbative parameter [26]. More details on the effective Hamiltonian approach can be found in Supplement 1.

As we are interested in intensity correlations, we can restrict our perturbative treatment of Eq. (3) to second order and truncate the Hilbert space at two excitations. In the following, for simplicity,

we also assume the plasmonic near-field, $\mathbf{E}_{SP}$, parallel to the laser field, $\mathbf{E}_L$ (as, for example, in particle-on-mirror cavities [16]). Moreover, we only consider the optimum configuration for strong coupling, in which $\boldsymbol{\mu}_{QE}$ is aligned with $\mathbf{E}_{SP}$. The scattering intensity, $I = \langle \hat{\mathbf{E}}_D^- \hat{\mathbf{E}}_D^+ \rangle$, is given within first-order perturbation theory as

$$I = (\eta N \mu_{SP} \Omega_{SP})^2 \left| \frac{\eta \tilde{\Delta}_{SP} + \tilde{\Delta}_{QE}/\eta N - 2\lambda}{\tilde{\Delta}_{SP}\tilde{\Delta}_{QE} - N\lambda^2} \right|^2, \tag{4}$$

where $\eta = \mu_{QE}/\mu_{SP} = \Omega_{QE}/\Omega_{SP}$, $\tilde{\Delta}_{SP} = \Delta_{SP} - i\gamma_{SP}/2$, and $\tilde{\Delta}_{QE} = \Delta_{QE} - i(\gamma_{QE}^{nr} + N\gamma_{QE}^{r})/2$. Using second-order perturbation theory, the correlation function, $g^{(2)}(0)$, can be expressed as

$$g^{(2)}(0) = \left| 1 - \frac{1}{N} \left( \frac{\eta \tilde{\Delta}_{SP} - \lambda}{\eta \tilde{\Delta}_{SP} + \tilde{\Delta}_{QE}/\eta N - 2\lambda} \right)^2 \frac{(\tilde{\Delta}_{QE} + iN\gamma_{QE}^{r}/2)[\tilde{\Delta}_{QE}\tilde{\Delta}_{SP} + (\tilde{\Delta}_{SP} - \lambda/\eta)^2 - N\lambda^2]}{(\tilde{\Delta}_{QE} + i\gamma_{QE}^{r}/2)[\tilde{\Delta}_{QE}\tilde{\Delta}_{SP} + \tilde{\Delta}_{SP}^2 - N\lambda^2] - \tilde{\Delta}_{SP}(N-1)\lambda^2} \right|^2. \tag{5}$$

Note that for $\gamma_{QE}^{nr} \gg \gamma_{QE}^{r}$, Eq. (5) yields $g^{(2)}(0) = (1 - 1/N)^2$ at $\lambda = 0$ and $\eta \to \infty$, recovering the flat correlation spectra in Fig. 2 for low-quantum-yield QE ensembles.

Figures 3(a)–3(d) render the far-field intensities (top row) and correlations (bottom row) for a nanocavity filled with four different QE ensembles $N = 1$, 5, 25, and 50, respectively. The horizontal and vertical axes correspond to laser frequency and QE–SP coupling strength, respectively. The latter is expressed through the single-emitter cooperativity, $C = 2\lambda^2/\gamma_{QE}\gamma_{SP}$, with upper limit $C = 2$ ($\lambda = 0.03$ eV), well below the collective ultrastrong coupling regime. We restrict our attention to QE–SP resonant coupling and consider the same parameters as in Fig. 2. Although the quantitative results shown in Fig. 3 depend on the specifics of the system, we have checked that our findings and their fundamental implications remain valid for a wide range of realistic configurations. As shown in Supplement 1, the behavior is also very similar when the SP field is spatially inhomogeneous or when inhomogeneous broadening is introduced for the QEs (note that the emitters cannot be formally described through a single bright state in these cases but must be treated individually). Dipole–dipole interactions among QEs are also analyzed in Supplement 1. Our results reveal that these have a significant impact on photon correlations in dense QE ensembles. Interestingly, we find that antibunching is more robust than bunching when interactions become large.

The complex $g^{(2)}(0)$ patterns in Figs. 3($a_2$)–3($d_2$) reveal that both photon bunching and antibunching occur in the strong coupling regime. These panels also show that the main quantum statistical features emerging at the single-emitter level (which are in qualitative agreement with recent experimental reports on semiconductor cavities [27,28]) are mostly retained as $N$ increases. Up to $N \sim 25$, photon emission is antibunched within a narrow frequency window located at $C \lesssim 1$, which implies that the single-emitter cooperativity can be considered as the key parameter determining photon correlations in ensembles containing up to several tens of QEs [29]. Notice also that, as a difference with high-quantum-yield QEs in low-loss semiconductor cavities, the inherent nonradiative losses of organic molecules and plasmonic systems allow observing antibunching for large $C$-values (see Supplement 1 for more details). On the other hand, bunched emission takes place at larger coupling strengths and within broader spectral domains for all $N$. Remarkably, there are spectral windows in which strong antibunching ($g^{(2)}(0) \approx 0$) takes place

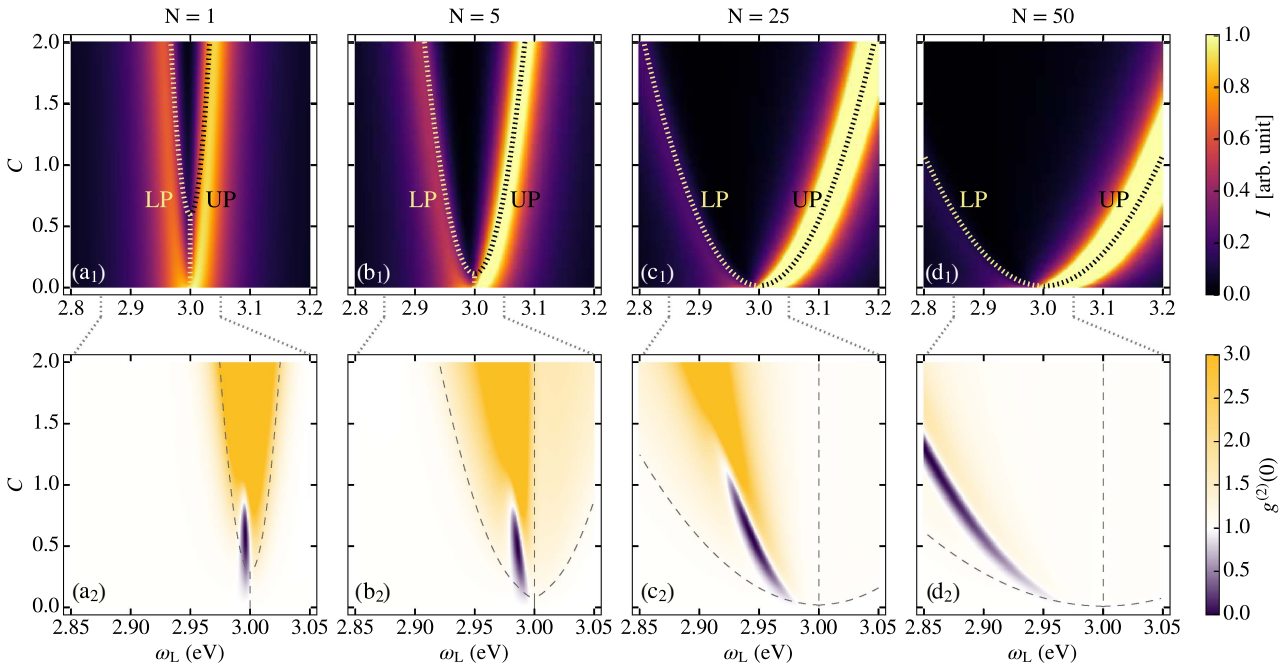


**Fig. 3.** ($a_1$)–($d_1$) Scattering intensity $I$ and ($a_2$)–($d_2$) correlation function $g^{(2)}(0)$ versus laser frequency and single emitter cooperativity for various QE–SP systems. In the upper (lower) panels dotted (dashed) lines plot the PEP frequencies (half-frequencies) in the one-excitation (two-excitation) manifold.

even for $N = 50$, whereas the emission from the uncoupled QE ensemble is essentially classical (see Fig. 2). This is the main result of this paper, namely, that in comparison to the uncoupled subsystems, collective plasmonic strong coupling can significantly enhance photon correlations in mesoscopic PEP systems.

By taking advantage of our analytical approach, we can gain physical insight into the results shown in Fig. 3. The intensity maps present two scattering maxima, whose origins lie at the denominator of Eq. (4). Its vanishing condition yields analytical expressions for the dispersion of the lower (LP) and upper (UP) PEPs in the first rung of the Tavis–Cummings ladder. These PEP frequencies, which naturally incorporate the $\sqrt{N}$ scaling characteristic of collective strong coupling, are plotted in dotted lines in top panels. Note that the intensity maxima overlap with the PEP dispersion bands, except for $N = 1$ and $C \lesssim 0.5$. This region, also perceptible for $N = 5$ at lower $C$, falls within the weak coupling regime, where Fano-like interferences between SP and QE emission gives rise to sharp scattering dips [30]. As $N$ increases, the contrast between UP (brighter) and LP (darker) scattering peaks increases. By introducing the PEP frequencies in the numerator of Eq. (4), the origin of this asymmetry becomes clear. Neglecting QE and SP damping, we obtain $I \propto (1 \mp \sqrt{N}\eta)^2$, where the upper (lower) sign must be used for LP (UP). Thus, QE and SP dipole moments are antiparallel along the LP dispersion, which diminishes $I$ as $N$ approaches $1/\eta^2$.

In a similar way as in the scattered intensity, we can expect that the vanishing of the denominator in the second term of Eq. (5) could give rise to nonclassical light. At $N = 1$, the resonant frequencies emerging from this condition are equal to half the energies of the LP (upper sign) and UP (lower sign) in the second rung of the Jaynes–Cummings ladder [31]. For $N > 1$, the same condition leads to a cubic equation: it accounts for the emergence of the middle PEPs in the two-excitation manifold (whose real half-frequency is equal to $\omega_{QE/SP}$). Moreover, notice the presence of the numerator of Eq. (4) in the denominator of the first factor in Eq. (5). As discussed above, this term acquires the form $(1 - \sqrt{N}\eta)$ at the LP band. Therefore, the darker character of LPs also makes them more suitable for photon correlations. PEP half-frequencies in the two-excitation manifold are plotted in dashed lines in Figs. 3($a_2$)–3($d_2$). The regions of strong photon correlations do not occur exactly at one of the polariton energies but slightly above the LP dispersion. This indicates that photon correlations, i.e., significant deviations from $g^{(2)}(0) = 1$, do not originate from transitions along a single PEP ladder but from the interference in the emission involving different hybrid states. This underlines the crucial role that strong coupling plays: while each PEP by itself is quasi-bosonic, the hybridization achieved through strong coupling ensures the coexistence of multiple mixed light–matter states separated by the Rabi splitting. It is the interference between the emission from these different but closely related states that leads to strongly nonclassical light emission.

In order to obtain a general view on the degree of bunching and antibunching attainable through QE–SP coupling, we evaluate Eq. (5) at its spectral maxima and minima. Figure 4 explore these extreme $g^{(2)}(0)$ values as functions of cooperativity and number of emitters. The inset renders overlapping maps for Max$[g^{(2)}(0)]$ (yellow) and Min$[g^{(2)}(0)]$ (violet), and the top and bottom panels plot cuts of these maps for various $C$-values. We can identify three domains according to the statistics of the scattered photons. For small QE ensembles and large $C$, only

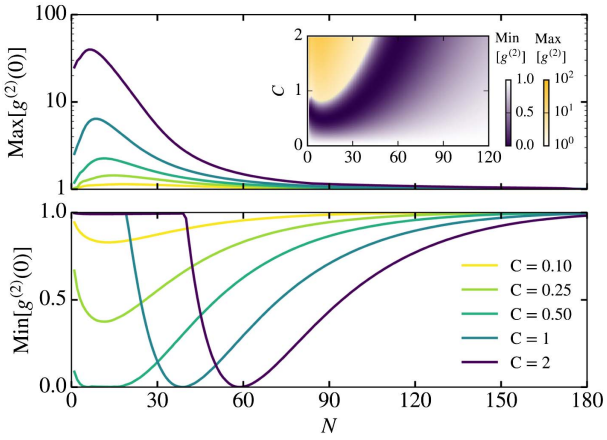


**Fig. 4.** Maximum (top) and minimum (bottom) correlation functions as functions of the QE ensemble size for several values of the single emitter cooperativity. The inset in the upper panel shows the map of photon positive (yellow) and negative (violet) correlations as functions of $N$ and $C$.

positive correlations take place, as in Figs. 3($a_2$)–3($c_2$) for $C > 1$. In this regime, Max$[g^{(2)}(0)]$ grows with increasing coupling strength and develops a maximum at $N \sim 10$ for all $C$. For very large $N$, a second domain is apparent. In this limit, PEPs bosonize as the $1/N$ factor in Eq. (5) governs $g^{(2)}(0)$, yielding maxima and minima approaching 1 monotonically as the number of QEs increases. Both bunched and antibunched emission takes place (within different spectral windows) at intermediate $N$ and $C$. In this third domain, positive correlations decay monotonically with $N$, whereas negative correlations are enhanced. Min$[g^{(2)}(0)]$ diminishes and reaches a minimum value, which corresponds to the lowest $g^{(2)}(0)$ achievable for a given $N$ and any $C$ (or *vice versa*). It can be proven that this minimum coincides with a sharp dip in the population of the plasmon state (written as a linear combination of PEPs) in the two-excitation manifold. In the limit of vanishing $\eta$ (which is a good approximation for our problem at small $N$), this condition simplifies to $C = \frac{\gamma_{QE}+\gamma_{SP}}{2\gamma_{SP}} \simeq \frac{1}{2}$. Figure 4 (bottom) shows this minimum developing with increasing cooperativity at $N \sim 10$ and reaching $g^{(2)}(0) = 0$ at $C = 0.5$. Remarkably, this zero in $g^{(2)}(0)$ shifts to larger $N$ for higher cooperativity, yielding strong photon antibunching at ensemble sizes as large as 100 QEs. Therefore, as anticipated in Fig. 3($d_2$), plasmonic strong coupling leads to the emergence of quantum nonlinearities in large excitonic systems, which would present $g^{(2)}(0) \simeq 1$ when not coupled to the plasmonic nanocavity.

## 4. CONCLUSION

We have investigated the complex photon statistics phenomenology that emerges from the strong coupling of a mesoscopic ensemble of quantum emitters and a single plasmon mode supported by a generic nanocavity. We have presented an analytical method describing the optical response of these systems under low-intensity coherent illumination. Our approach provides insights into the role that both the plasmon-exciton-polariton ladder and its tuning through the single emitter cooperativity play in the emission of strongly correlated (bunched and/or antibunched) light. Finally, our results demonstrate the robustness of these compound systems against bosonization effects, predicting strong

intensity correlations at considerable ensemble sizes. Our theoretical findings demonstrate the feasibility and establish experimental guidelines toward the realization of nanoscale nonclassical light sources operating beyond the single-emitter level.

**Funding.** FP7 Ideas: European Research Council (IDEAS-ERC) (ERC-2011-AdG 290981, ERC-2016-STG-714870, FP7-PEOPLE-2013-CIG-618229, FP7-PEOPLE-2013-CIG-630996); Ministerio de Economía y Competitividad (MINECO) (FIS2015-64951-R, MAT2014-53432-C5-5-R, MDM-2014-0377).

See Supplement 1 for supporting content.

## REFERENCES

1. P. Törmä and W. L. Barnes, "Strong coupling between surface plasmon polaritons and emitters: a review," Rep. Prog. Phys. **78**, 013901 (2015).
2. J. Bellessa, C. Bonnand, J. C. Plenet, and J. Mugnier, "Strong coupling between surface plasmons and excitons in an organic semiconductor," Phys. Rev. Lett. **93**, 036404 (2004).
3. T. Schwartz, J. A. Hutchison, C. Genet, and T. W. Ebbesen, "Reversible switching of ultrastrong light–molecule coupling," Phys. Rev. Lett. **106**, 196405 (2011).
4. A. González-Tudela, P. A. Huidobro, L. Martín-Moreno, C. Tejedor, and F. J. García-Vidal, "Theory of strong coupling between quantum emitters and propagating surface plasmons," Phys. Rev. Lett. **110**, 126801 (2013).
5. A. Delga, J. Feist, J. Bravo-Abad, and F. J. García-Vidal, "Quantum emitters near a metal nanoparticle: strong coupling and quenching," Phys. Rev. Lett. **112**, 253601 (2014).
6. G. Zengin, M. Wersäll, S. Nilsson, T. J. Antosiewicz, M. Käll, and T. Shegai, "Realizing strong light–matter interactions between single-nanoparticle plasmons and molecular excitons at ambient conditions," Phys. Rev. Lett. **114**, 157401 (2015).
7. F. Todisco, S. D'Agostino, M. Esposito, A. I. Fernández-Domínguez, M. De Giorgi, D. Ballarini, L. Dominici, I. Tarantini, M. Cuscuna, F. Della Sala, G. Gigli, and D. Sanvitto, "Exciton–plasmon coupling enhancement via metal oxidation," ACS Nano **9**, 9691–9699 (2015).
8. J. A. Hutchison, T. Schwartz, C. Genet, E. Devaux, and T. W. Ebbesen, "Modifying chemical landscapes by coupling to vacuum fields," Angew. Chem. **124**, 1624–1628 (2012).
9. J. Galego, F. J. García-Vidal, and J. Feist, "Cavity-induced modifications of molecular structure in the strong-coupling regime," Phys. Rev. X **5**, 041022 (2015).
10. E. Orgiu, J. George, J. A. Hutchison, E. Devaux, J. F. Dayen, B. Doudin, F. Stellacci, C. Genet, J. Schachenmayer, C. Genes, G. Pupillo, P. Samorì, and T. W. Ebbesen, "Conductivity in organic semiconductors," Nat. Mater. **14**, 1123–1129 (2015).
11. J. Feist and F. J. García-Vidal, "Extraordinary exciton conductance induced by strong coupling," Phys. Rev. Lett. **114**, 196402 (2015).
12. T. K. Hakala, H. T. Rekola, A. I. Väkeväinen, J.-P. Martikainen, M. Nečada, A. J. Moilanen, and P. Törmä, "Lasing in dark and bright modes of a finite-sized plasmonic lattice," Nat. Commun. **8**, 13687 (2017).
13. M. Ramezani, A. Halpin, A. I. Fernández-Domínguez, J. Feist, S. R.-K. Rodriguez, F. J. García-Vidal, and J. Gómez-Rivas, "Plasmon-exciton-polariton lasing," Optica **4**, 31–37 (2017).
14. M. S. Tame, K. R. McEnery, S. K. Özdemir, J. Lee, S. A. Maier, and M. S. Kim, "Quantum plasmonics," Nat. Phys. **9**, 329–340 (2013).
15. T. Holstein and H. Primakoff, "Field dependence of the intrinsic domain magnetization of a ferromagnet," Phys. Rev. **58**, 1098–1113 (1940).
16. R. Chikkaraddy, B. de Nijs, F. Benz, S. J. Barrow, O. A. Scherman, E. Rosta, A. Demetriadou, P. Fox, O. Hess, and J. J. Baumberg, "Single-molecule strong coupling at room temperature in plasmonic nanocavities," Nature **535**, 127–130 (2016).
17. K. Santhosh, O. Bitton, L. Chuntonov, and G. Haran, "Vacuum Rabi splitting in a plasmonic cavity at the single quantum emitter limit," Nat. Commun. **7**, 11823 (2016).
18. R.-Q. Li, D. Hernangómez-Pérez, F. J. García-Vidal, and A. I. Fernández-Domínguez, "Transformation optics approach to plasmon-exciton strong coupling in nanocavities," Phys. Rev. Lett. **117**, 107401 (2016).
19. M. Tavis and F. W. Cummings, "Exact solution for an N-molecule-radiation-field Hamiltonian," Phys. Rev. **170**, 379–384 (1968).
20. M. O. Scully and M. S. Zubairy, *Quantum Optics* (Cambridge University, 1997).
21. B. R. Mollow, "Power spectrum of light scattered by two-level systems," Phys. Rev. **188**, 1969–1975 (1969).
22. F. Miftasani and P. Machnikowski, "Photon–photon correlation statistics in the collective emission from ensembles of self-assembled quantum dots," Phys. Rev. B **93**, 075311 (2016).
23. A. Auffeves, D. Gerace, S. Portolan, A. Drezet, and M. França Santos, "Few emitters in a cavity: from cooperative emission to individualization," New J. Phys. **13**, 093020 (2011).
24. A. N. Poddubny, M. M. Glazov, and N. S. Averkiev, "Nonlinear emission spectra of quantum dots strongly coupled to a photonic mode," Phys. Rev. B **82**, 205330 (2010).
25. P. M. Visser and G. Nienhuis, "Solution of quantum master equations in terms of a non-Hermitian Hamiltonian," Phys. Rev. A **52**, 4727–4736 (1995).
26. R. J. Brecha, P. R. Rice, and M. Xiao, "N two-level atoms in a driven optical cavity: quantum dynamics of forward photon scattering for weak incident fields," Phys. Rev. A **59**, 2392–2417 (1999).
27. K. Müller, A. Rundquist, K. A. Fisher, T. Sarmiento, K. G. Lagoudakis, Y. A. Kelaita, C. Sánchez-Muñoz, E. del Valle, F. P. Laussy, and J. Vučković, "Coherent generation of nonclassical light on chip via detuned photon blockade," Phys. Rev. Lett. **114**, 233601 (2015).
28. A. Faraon, I. Fushman, D. Englund, N. Stoltz, P. Petroff, and J. Vučković, "Coherent generation of non-classical light on a chip via photon-induced tunnelling and blockade," Nat. Phys. **4**, 859–863 (2008).
29. H. Habibian, S. Zippilli, and G. Morigi, "Quantum light by atomic arrays in optical resonators," Phys. Rev. A **84**, 033829 (2011).
30. A. Ridolfo, O. Di Stefano, N. Fina, R. Saija, and S. Savasta, "Quantum plasmonics with quantum dot-metal nanoparticle molecules: influence of the Fano effect on photon statistics," Phys. Rev. Lett. **105**, 263601 (2010).
31. F. P. Laussy, E. del Valle, M. Schrapp, A. Laucht, and J. J. Finley, "Climbing the Jaynes–Cummings ladder by photon counting," J. Nanophoton. **6**, 061803 (2012).